IEEE Photonics Journal
An IEEE Photonics Society Publication

Ultrasonic Modulation of Coherent Light in Raman–Nath Diffraction

Volume 10, Number 5, September 2018

Weng Cuncheng
He Youwu

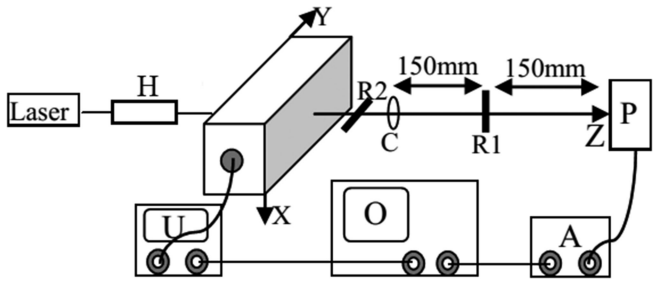

DOI: 10.1109/JPHOT.2018.2865438
1943-0655

IEEE photonics SOCIETY

IEEE

Ultrasonic Modulation of Coherent Light in Raman–Nath Diffraction

Weng Cuncheng [1,2,3] **and He Youwu** [2]

[1]College of Physics and Energy, Fujian Provincial Key Laboratory of Quantum Manipulation and New Energy Materials, Fujian Normal University, Fuzhou 350007, China
[2]Key Laboratory of Optoelectronic Science and Technology for Medicine of Ministry of Education, Fujian Provincial Key Laboratory of Photonics Technology,Fujian Provincial Engineering Technology Research Center of Photoelectric Sensing Application, Fujian Normal University, Fuzhou 350007, China
[3]Fujian Provincial Collaborative Innovation Center for Optoelectronic Semiconductors and Efficient Devices, Xiamen 361005, China

DOI:10.1109/JPHOT.2018.2865438

Manuscript received June 28, 2018; revised July 29, 2018; accepted August 10, 2018. Date of publication August 14, 2018; date of current version August 24, 2018. This work was supported in part by the National Natural Science Foundation of China (61575043); in part by the Special Funds of the Central Government Guiding Local Science and Technology Development (2017L3009); and in part by the Science and Technology program of the Educational Office of Fujian Province of China (JAT170124).
Corresponding author: He Youwu (e-mail: ywhe@fjnu.edu.cn).

Abstract: This paper analyzes the ultrasonic modulation of coherent light in Raman–Nath acousto-optic diffraction. We find that the frequency shifts of the diffracted light cause the periodic variation of the ultrasound-modulated light intensity with time. Additionally, the phase shifts of the diffracted light result in the periodic variation of the ultrasound-modulated light intensity along the ultrasound beam.

Index Terms: Acousto-optic modulation, optical phase shift, optical frequency shift.

1. Introduction

Ultrasound-Modulated optical tomography is a hybrid technique that combines ultrasound and optics [1]–[8]. In the tomography, an ultrasound wave is focused into a medium to modulate coherent light passing through the ultrasonic field. The ultrasonic modulation causes the intensity of coherent light escaping from the ultrasonic field to vary periodically with the ultrasonic frequency. The light of which the intensity varies periodically with the ultrasonic frequency is called the ultrasound-modulated light. This temporal variation has been considered to be due to the optical phase modulation resulting from the ultrasound-induced displacement of scatterers and the ultrasonic modulation of the refractive index in the ultrasonic field [1]–[8]. The optical phase modulation means that the optical path of the incident light in the ultrasonic field is modulated by the ultrasound. Consequently, optical phase modulation has been considered to be the effect responsible for the periodic variation of the ultrasound-modulated light intensity with time [1]–[8].

In an optically transparent medium, ultrasonic action produces a travelling phase-grating, which causes diffractions of incident light [9]–[14]. The diffractions are divided into two distinct diffraction types: Raman-Nath and Bragg diffractions. Traditionally, the type of diffraction is determined by the conditions $Q << 1$ and $Q >> 1$, respectively [9], [12], [13]. The Q is the Klein Cook parameter. Here, only Raman-Nath diffraction (RNd) is concerned. The features of RNd are short interaction

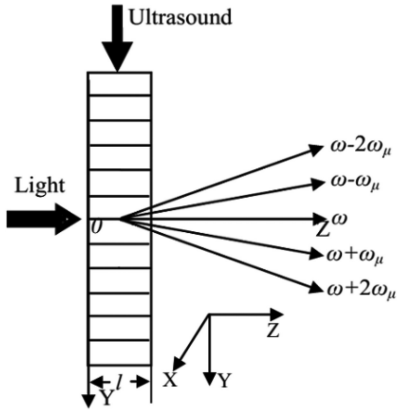

Fig. 1. Representation of the ultrasound–light interaction in RNd.

length and multi-order diffractions; therefore, RNd has been still considered as a moving thin phase grating diffraction [9]–[14]. In RNd, the ultrasonic action causes frequency and phase shifts of the diffracted light.

This paper studies the ultrasonic modulation of coherent light in Raman–Nath diffraction (RNd). Our theoretical and experimental studies show that the frequency shifts of the diffracted light cause also the periodic variation of the ultrasound-modulated light intensity with time. They also show that the phase shifts of the diffracted light result in the periodic variation of the ultrasound-modulated light intensity along the ultrasound beam.

2. Theory

The RNd ultrasonic modulation to be considered here is two-dimensional, as seen in Figure 1. An idealized longitudinal ultrasound wave traveling in the Y-direction with angular frequency ω_μ is contained between the planes z = 0 and z = l in an optically transparent medium of refractive index n_0. A plane light wave of unit amplitude is assumed to impinge upon the acoustically produced grating along the Z-axis. The temporal and spatial modulation of the refractive index in the ultrasonic field can then be written as [4]–[6], [9]–[12]

$$n\,(t, y) = n_0 + \Delta n \sin\omega_\mu \left(t + \frac{y}{v}\right), \tag{1}$$

where Δn is the amplitude of the refractive index change and v is the ultrasound velocity in the medium.

The incident light entering the ultrasonic field will be diffracted, with the qth-order diffracted light $Eq(t, y, l)$ obeying [4]–[6], [9]–[12]

$$E_q\,(t, y, l) = J_q(\varphi)\exp j\left[-\left(\omega + q\omega_\mu\right) t + kn_0 l + \frac{q\omega_\mu y}{v}\right], \tag{2}$$

where q is an integer, $\varphi = k\Delta nl$, J_q () denotes the qth-order Bessel function, ω is the angular frequency of the incident light, and k is the wave vector of the incident light in vacuum.

From Eq. (2), the qth-order diffracted light is frequency-shifted by $q\omega_\mu$ and phase-shifted by $q\omega_\mu y/v$ [9]–[14]

To show the periodic variation of the ultrasound-modulated light intensity along the ultrasound beam, only the ultrasound-modulated light coming from a defined region in the ultrasonic field is collected. This region, centered at (0, y, 0), is assumed to be a rectangle with lengths 2a and 2d along the X- and Y-directions, respectively.

Considering the collection of only the zero- and first-order light diffracted from the defined region, the collected light intensity is given by Eq. (3)

$$\begin{aligned} I_{01}(t,y) &= \int_{-a}^{a} dx \int_{y-b}^{y+b} dy \left| \left\{ \left[J_0(\varphi) + J_1(\varphi) \text{exp}j\left(-\omega_\mu t + \frac{\omega_\mu y}{v}\right)\right]\right\} \text{exp}j\left(-\omega t + kn_0 l\right)\right|^2 \\ &= 2a \int_{y-b}^{y+b} \left[J_0^2(\varphi) + J_1^2(\varphi) + 2J_0(\varphi)J_1(\varphi)\cos\omega_\mu\left(t - \frac{y}{v}\right)\right] dy \\ &= 4ab\left[J_0^2(\varphi) + J_1^2(\varphi) + \frac{v\sin\left(\frac{\omega_\mu b}{v}\right)}{\omega_\mu b} J_0(\varphi)J_1(\varphi)\cos\omega_\mu\left(t - \frac{y}{v}\right)\right], \end{aligned} \tag{3}$$

which shows that the collected light intensity is a function of cos[$\omega_\mu(t - y/v)$] and, therefore, varies periodically with time and along the Y-direction (the direction of the ultrasound beam). Additionally, the optical frequency shifts are responsible for the periodic variation of the collected light intensity with time. The optical phase shifts are then responsible for causing the periodic variation of the collected light intensity along the ultrasound beam. The amplitude of the collected light intensity A_{01} can be written as

$$A_{01} = \frac{4avJ_0(\varphi)J_1(\varphi)\sin\left(\frac{\omega_\mu b}{v}\right)}{\omega_\mu}. \tag{4}$$

Considering the collection of only the qth and $(q+1)$th-order light diffracted from the defined region, the collected light intensity is given by Eq. (5)

$$\begin{aligned} I_{qq+1}(t,y) &= \int_{-a}^{a} dx \int_{y-b}^{y+b} dy \left| \left[J_q(\varphi)\text{exp}jq\left(-\omega_\mu t + \frac{\omega_\mu y}{v}\right) + J_{q+1}(\varphi)\text{exp}j(q+1)\left(-\omega_\mu t + \frac{\omega_\mu y}{v}\right)\right]\right. \\ &\quad \left.\text{exp}j\left(-\omega t + kn_0 l\right)\right|^2 \\ &= 2a \int_{y-b}^{y+b} \left[J_q^2(\varphi) + J_{q+1}^2(\varphi) + 2J_q(\varphi)J_{q+1}(\varphi)\cos\omega_\mu\left(t - \frac{y}{v}\right)\right] dy \\ &= 4ab\left[J_q^2(\varphi) + J_{q+1}^2(\varphi) + \frac{v\sin\left(\frac{\omega_\mu b}{v}\right)}{\omega_\mu b} J_q(\varphi)J_{q+1}(\varphi)\cos\omega_\mu\left(t - \frac{y}{v}\right)\right], \end{aligned} \tag{5}$$

which shows that the collected light intensity is also a function of cos $[\omega_\mu(t - y/v)]$, and therefore varies periodically both with time and along the Y-direction. Finally, considering the collection of all orders of light diffracted from the defined region, the collected light intensity is given by Eq. (6), where p is an integer.

$$\begin{aligned} I(t,y) &= \int_{-a}^{a} dx \int_{y-b}^{y+b} \left| \sum_{q=-\infty}^{\infty} J_q(\varphi)\text{exp}j\left[-\left(\omega + q\omega_\mu\right)t + kn_0 l + \frac{q\omega_\mu y}{v}\right]\right|^2 dy \\ &= 2a \int_{y-b}^{y+b} \left\{ \sum_{q=-\infty}^{\infty} J_q^2(\varphi) + 2\sum_{p\neq q} J_p(\varphi)J_q(\varphi)\cos\left[\left(p - q\right)\omega_\mu\left(t - \frac{y}{v}\right)\right]\right\} dy \end{aligned} \tag{6}$$

According to Eq. (3), Eq. (6) can be simplified to

$$I(t,y) = 4ab\sum_{q=0}^{\infty} M_q \cos q\omega_\mu\left(t - \frac{y}{v}\right), \tag{7}$$

where M_q is a constant. Note that the collected light intensity is also a function of cos $[q\omega_\mu(t - y/v)]$ and, therefore, varies periodically both with time and along the Y-direction. Note further that the

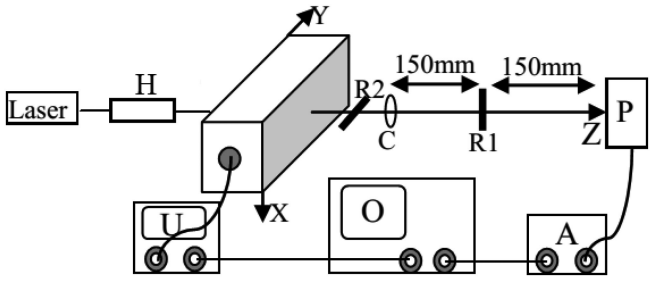

Fig. 2. Schematic diagram of the experimental setup. U: ultrasonic transducer and its driver; O: digital oscilloscope; A: amplifier; P: photomultiplier; R: rectangular slit; C: convex lens; H: collimator.

intensity signals can be considered to be composed of a series of cosine signals with frequencies that are integer multiples of the ultrasonic frequency.

3. Experiment

To verify the above analysis, an experimental setup with two rectangular slits was used (see Figure 2). Slit R1 measured 15 mm along the X-direction, and could be adjusted along the Y-direction. Slit R2 measured 15 mm along the Y-direction, and approximately 1 mm along the X-direction. A convex lens was also used, with focal length of 150 mm and 25-mm aperture. A function generator was used to create a sinusoidal electrical signal, which was then applied to an unfocusing transducer to generate a continuous ultrasound wave with a frequency of 1.71 MHz. The ultrasound beam, with a diameter of 1.7 cm, propagated into distilled water along the Y-direction. The distances from the central axis of the ultrasound beam to the lower and left surfaces of the tank were approximately 3.5 cm and 2.5 cm, respectively. The tank, whose dimensions were 7.0, 9.0, and 5.0 cm along the X-, Y-, and Z-directions, respectively, contained 270 ml of distilled water. A 630-nm laser light with a 4-mm diameter was focused into a collimator with an incident small hole with a diameter of 0.05 mm and then irradiated the tank. The distance from the collimator to the tank was approximately 3.0 cm. The light wave escaping from the collimator becomes a plane light beam with a 2-cm diameter. The optical signal escaping from the tank and then passing through R2, C, and R1 was collected by a photomultiplier (PMT) with a rectangular incident window. The distances from R2 to the tank and C were approximately 3.0 cm and 2.0 cm, respectively. The distances from R1 to C and the PMT were 150 mm. The diffracted light escaping from C converged to the focal plane of C. The rectangular incident window was 2.0 mm along the X-direction and could be adjusted along the Y-direction. The optical signal coming from the PMT was read by an oscilloscope, after being amplified. The PMT could be moved in the Y-direction. The electrical signal exciting the transducer was also read with an oscilloscope, and was chosen as reference. An ultrasonic absorber was placed behind the distilled water.

The value of Q [9], [13] was approximately 0.069, and therefore, the optical diffraction was RNd. Additionally, because the ultrasound beam was columnar, R2 was used, so that the interaction length of the ultrasound and the collected light could be considered to be the same. The ultrasonic wavelength in distilled water was of only 0.854 mm; therefore, the ultrasound wave (1.7-cm diameter) could be approximately considered as a plane wave. Finally, the incident window of the PMT was setup so that only the diffracted light coming from a region in the ultrasonic field was collected.

Because the ultrasound beam was columnar, the interaction length l of the ultrasound and the collected light is a function of x. However, according to Eqs. (3), (5) and (6), the temporal and spatial variations of the collected light intensity were not dependent on x. Consequently, the optical diffraction of R2 along the X-direction can be ignored when showing the temporal and spatial variations.

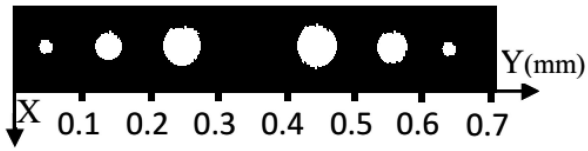

Fig. 3. Distributions of the diffracted light in the focal plane of C.

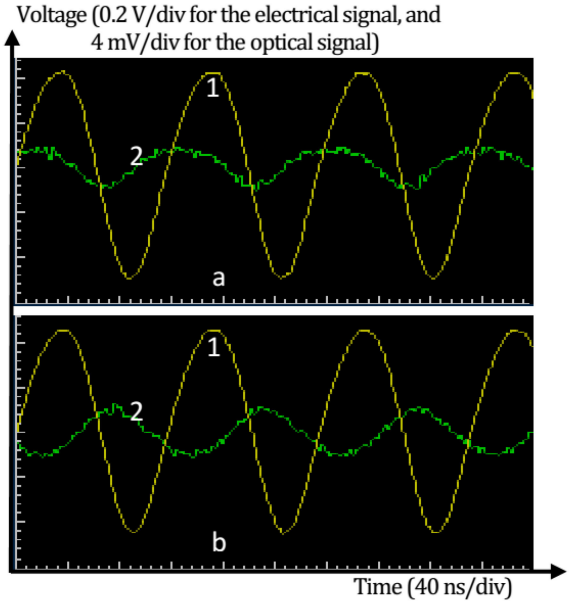

Fig. 4. Periodic variations of the collected light intensity with time and along the Y-direction. Curve 1 is the electrical signal applied to the transducer, and curve 2 is the optical signal output by the PMT. (a) Initial PMT position. (b) PMT shifted about 0.410 mm along the Y-direction.

To collect the diffracted light, both C and R1 were used. The diffracted light escaping from R2 was made to converge onto the plane of R1 by C, and was then selectively collected by R1, based on a spatial filtering technique.

The amplitude of the electrical signal applied to the ultrasonic transducer was adjusted until the zero-order diffracted light was made to disappear, a condition in which the electrical signal amplitude was approximately 9.6 V, and $J_q(\varphi) = 0$; the distributions of the diffracted light in the focal plane of C were obtained with a charge-coupled-device, and are shown in Figure 3. The experiment showed that the diffracted lights of different orders were well separated. Consequently, we could choose which diffracted light to collect by R1. Additionally, for an electrical signal amplitude of 9.6 V, the value of φ was 2.4.

Only zero- and first-order diffracted light was collected. The amplitude of the electrical signal exciting the transducer remained at approximately 2.4 V. The size of the PMT incident window was maintained at approximately 0.4 mm along the Y-direction. Figure 4(a) showed the waveforms of the electrical and optical signals observed with the oscilloscope. As shown, the collected light intensity varied periodically with time.

According to Eqs. (3) and (5), the collected light intensity varies along the Y-direction with a period equal to the ultrasonic wavelength in the medium. To show this spatial variation, the PMT was moved in the Y-direction; the results are shown in Figure 4(b). We observe that the electrical signal waveform remains still, while the optical signal waveform shifts along the time axis, with both overlapping periodically. Using the double trace method, the period of spatial variation was

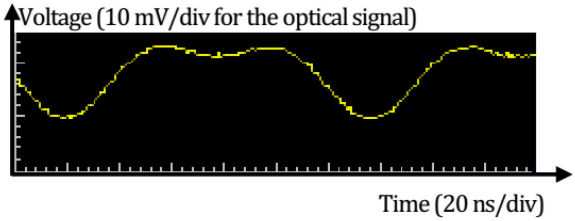

Fig. 5. Optical signal waveforms obtained at the oscilloscope when collecting all orders of diffracted light.

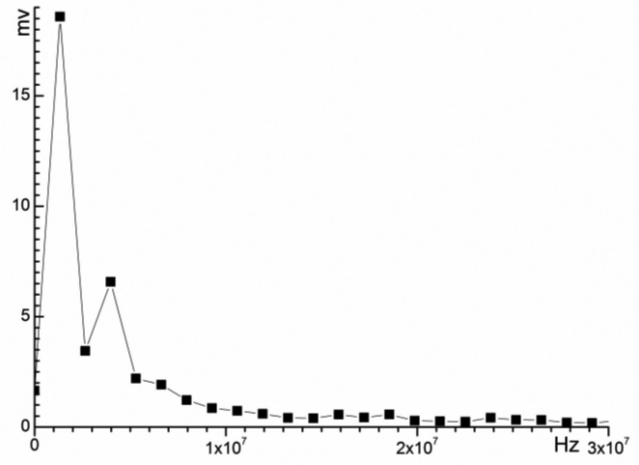

Fig. 6. Fourier transform of the signal waveform in Figure 5.

measured and found to be of 0.854 ± 0.016 mm. At room temperature, the ultrasonic velocity is about 1480 m/s in pure water, which means that, for the 1.71 MHz ultrasound wave, the wavelength was approximately equal to 0.865 mm. Clearly, the period of spatial variation is equal to the ultrasonic wavelength within the error range. The experiment confirmed the temporal and spatial variations in the collected light intensity, which has also been observed before [15].

The size of the PMT incident window was sequentially adjusted to 0.5, 0.7, 0.9, and 1.2 mm, and the previous experiment was repeated at each step. The same periodic overlapping was observed. Consequently, the optical diffraction of the incident window can be ignored when showing the temporal and spatial variations. Additionally, it is adequate to focus on the defined region in order to show the temporal and spatial variations.

The above experiment was then repeated, but this time collecting only first- and second-order diffracted light. The same periodic overlapping was again observed. This overlap period was again measured and was 0.856 ± 0.018 mm. The experiment confirmed the temporal and spatial variations, too.

Both C and R1 were then removed, so that all orders of diffracted light would be collected, and the above experiment was repeated. The periodic overlapping was once again observed. The experiment further confirmed the temporal and spatial variations in the collected light intensity. Additionally, the optical diffraction of R1 can be ignored when showing the temporal and spatial variations. Figure 5 shows the collected light intensity signal waveform obtained at the oscilloscope; the PMT incident window size remained at approximately 0.4 mm along the Y-direction. Figure 6 shows the Fourier transform of the waveform in Figure 5. We note that the intensity signals are mainly composed of cosine signals with angular frequencies of ω_μ and $2\omega_\mu$. The experimental results therefore confirm Eq. (7).

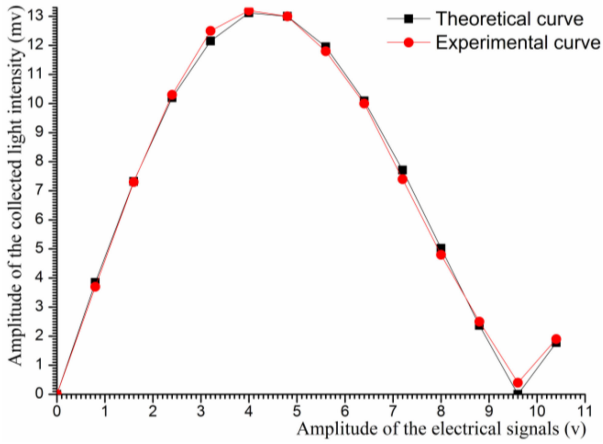

Fig. 7. Amplitude of the collected light intensity as a function of the amplitude of the electrical signal exciting the transducer.

Both C and R1 were not removed. Only zero- and first-order diffracted light was once again collected. The size of the PMT incident window remained at approximately 0.4 mm along the Y-direction. Figure 7 shows the amplitude of the collected light intensity as a function of the amplitude of the electrical signal exciting the transducer. In this figure we also represented the theoretical curve, as given by Eq. (4). The agreement between Eq. (4) and the obtained experimental results is clear, which further validates the equation.

4. Discussion and Conclusion

It is well known that the optical heterodyne technique uses the coherent superposition of frequency-shifted light and a reference to produce periodical variations of light intensity at the frequency of the frequency shift. In RNd, the diffracted light is frequency-shifted at each order by different integer multiples of the ultrasonic frequency. Consequently, the coherent superposition of the diffracted light must cause the superposition intensity to vary periodically with time, and the superposition signals can be considered to be composed of a series of cosine signals whose frequencies are different multiples of the ultrasonic frequency.

We know that the superposition intensity of two beams of coherent light depends on their phase differences. In RNd, the phase of the diffracted light is a linear function of y (the origin of diffracted light in the ultrasonic field). Consequently, the coherent superposition intensity of the diffracted light varies periodically along the ultrasound beam.

In ultrasound-modulated optical tomography, the ultrasonic modulation causes the ultrasound-modulated light intensity to vary periodically with time. The temporal variation has been considered to be due to the optical phase modulation. However, in this paper, by analyzing the ultrasonic modulation of coherent light in RNd, we find that the frequency shifts of the diffracted light can also cause the periodic variation of the ultrasound-modulated light intensity with time. Additionally, we find that the phase shifts of the diffracted light result in the periodic variation of the ultrasound-modulated light intensity along the ultrasound beam.

References

[1] L.-H. Wang, “Mechanisms of ultrasonic modulation of multiply scattered coherent light: An analytic model,” *Phys. Rev. Lett.*, vol. 87, 2001, Art. no. 043903.
[2] M. Gross, “Selection of the tagged photons by off axis heterodyne holography in ultrasound-modulated optical tomography,” *Appl. Opt.*, vol. 56, pp. 1846–1854, 2017.

[3] M. Lesaffre, S. Farahi, M. Gross, P. Delaye, A. C. Boccara, and F. Ramaz, "Acousto-optical coherence tomography using random phase jumps on ultrasound and light," *Opt. Exp.*, vol. 17, pp. 18211–18218, 2009.
[4] K. Zhu, Y. Lu, S. Zhang, H. Ruan, S. Usuki, and Y. Tan, "Ultrasound modulated laser confocal feedback imaging inside turbid media," *Opt. Lett.*, vol. 43, pp. 1207–1210, 2018.
[5] E. B. Guillaume, U. Bortolozzo, J.-P. Huignard, S. Residori, and F. Ramaz, "Dynamic ultrasound modulated optical tomography by self-referenced photorefractive holography," *Opt. Lett.*, vol. 38, pp. 287–289, 2013.
[6] Y. Liu, Y. Shen, C. Ma, J. Shi, and L. V. Wang, "Lock-in camera based heterodyne holography for ultrasound-modulated optical tomography inside dynamic scattering media," *Appl. Phys. Lett.*, vol. 108, 2016, Art. no. 231106.
[7] P. Lai, X. Xu, and L. V. Wang, "Ultrasound-modulated optical tomography at new depth," *J. Biomed. Opt.*, vol. 17, pp. 176–177, 2012.
[8] Y. Suzuki, P. Lai, X. Xu, and L. Wang, "High-sensitivity ultrasound-modulated optical tomography with a photorefractive polymer," *Opt. Lett.*, vol. 38, pp. 899–901, 2013.
[9] R. W. Boyd, *Nonlinear Optics*, 3rd ed. New York, NY, USA: Academic, 2008, ch. 8.
[10] G. Gondek, T. Katkowski, and P. Kwiek, "Near field of light diffracted by an ultrasonic wave, beyond the Raman Nath diffraction regime," *Opt. Eng.*, vol. 38, pp. 1102–1107, 1999.
[11] E. Blomme and O. Leroy, "Plane-wave analysis of the near field of light diffracted by ultrasound," *J. Acoust. Soc. Amer.*, vol. 91, pp. 1474–1483, 1992.
[12] W. R. Klein and B. D. Cook Klein, "Unified approach to ultrasonic light diffraction," *IEEE Trans. Sonics Ultrason.*, vol. 14, no. 3, pp. 123–134, Jul. 1967.
[13] K. A. I. L. W. Gamalath and G. L. A. U. Jayawardena, "Diffraction of light by acoustic waves in liquids," *Int. Lett. Chem., Phys. Astron.*, vol. 39, pp. 39–57, 2012.
[14] Q. Zhao, S. He, B. J. Li, P.-L. Liu, and X. Dong, "Two-dimensional Raman–Nath acousto-optic bistability by use of frequency feedback," *Appl. Opt.*, vol. 36, pp. 2408–2413, 1997.
[15] C. Weng and X. Zhang, "Model of Raman–Nath acousto-optic diffraction," *Chin. Opt. Lett.*, vol. 13, 2015, Art. no. 101701.